DETERMINING FACTORS THAT INFLUENCE TURBIDITY IN KANEOHE BAY, OAHU

A THESIS SUBMITTED TO
THE GLOBAL ENVIRONMENTAL SCIENCE
UNDERGRADUATE DIVISION IN PARTIAL FULFILLMENT
OF THE REQUIREMENTS FOR THE DEGREE OF

BACHELOR OF SCIENCE WITH HONORS

IN

GLOBAL ENVIRONMENTAL SCIENCE

SUMMER 2006

By
Everett H. Ohta

Thesis Advisor
Geno Pawlak

I certify that I have read this thesis and that, in my opinion, it is satisfactory in scope and quality as a thesis for the degree of Bachelor of Science in Global Environmental Science.

THESIS ADVISOR

_____

Geno Pawlak

Department of Ocean and Resources Engineering

Acknowledgements

I would like to express my appreciation for the support from my family and friends throughout the years. Special thanks also go out to my thesis advisor, Geno Pawlak, for his assistance and guidance throughout this project, from which I have learned so much.

I would like to acknowledge Ryan Lowe and Jim Falter for the use of their Kaneohe ADCP data. Also, thank you to the numerous individuals that have helped me throughout the various stages of this project: Eric De Carlo, Margaret McManus, the members of the Environmental Fluid Dynamics Lab (Marion Bandet-Chavanne, Mindy Swanson, Andy Hebert, Kimball Millikan, Judith Wells, and Joseph Shacat), Frank Sansone, Kuulei Rodgers, Tyson Hilmer, Chris Ostrander, Laura deGelleke, Chris Colgrove, and to the faculty and staff of the Global Environmental Science program.

Abstract

In recent years, much attention has been given to suspended particulate matter (SPM) concentrations, or suspended load, due to its potential impact on reef ecosystems. Solids are transported through the ocean and can have both detrimental (through sedimentation) and beneficial (supplying nutrients) effects on a coral reef community.

This project seeks to identify the marine physical mechanisms that influence SPM concentrations in the reef environment of Kaneohe Bay. An acoustic Doppler current profiler (ADCP) was used to measure a number of water properties over the coral reef that extends across the mouth of Kaneohe Bay. The benefit of the ADCP is that it allows researchers to not only measure water current velocities throughout the entire water column, but it also enables this sampling to occur over extended periods of time.

Sampling occurred during three separate deployments. The third ADCP deployment occurred in conjunction with field sampling with a Niskin bottle in hopes of calibrating measured ADCP values of acoustic backscatter with SPM concentration from filtered samples.

Analysis of the ADCP data showed significant variation in the echo intensity (EI) signal, which can be used as an analogue for turbidity, between the ADCP sites. Current speed and wave height exhibited a covariant relationship with EI data, with higher EI values typically associated with higher waves and faster currents. Surprisingly, Sites 0-2 exhibited a diurnal cycle in EI levels, suggesting that marine biota may constitute a significant portion of the scatterers responsible for the EI data. It was not possible to confirm this hypothesis however, due to minimal data regarding the actual composition of the SSC at the time of deployments. The strongest relationship was found to be the EI response to vertical current velocities, themselves exhibiting a diurnal cycle. This relationship was not present at Site 3. The mechanism for vertical currents appears to be related to the incoming tide. There was a poor correlation between EI, as measured by the ADCP, and the filtered water samples from the third experiment. This was likely due to high spatial variations in reef characteristics and the inherent difficulty in measuring relatively small changes in suspended load.

TABLE OF CONTENTS

List of Figures

Chapter 1: Introduction

Suspended particulate matter (SPM) concentration has been given much attention in recent research, owing to its effect on the offshore reef environment. SPM concentrations in a volume of water contribute to a water sample's turbidity. In many instances, it has been shown that turbidity can have a deleterious effect on coral growth due to its limiting effect on light inputs and burial of living corals (Grigg and Dollar, 1990). Another concern for researchers and policymakers alike has been the damage that humans may impart through urban discharge to the shore. Due to difficulties in estimation of a turbidity response threshold, one may begin protection efforts by characterizing the natural state of the reef and the processes that contribute to elevated levels of turbidity (Orpin et al. 2004).

Early measurements of suspended sediment loads in the water column employed sampling instruments, such as Niskin bottles, to obtain a water sample at a specific depth in the water column (Holdaway et al., 1999). Although it is possible to use such sampling bottles in series to obtain measurements over the water column, they cannot provide insight into temporal variations in turbidity without numerous deployments. Many researchers have thus turned to optical and acoustic instruments to estimate SPM concentrations over extended periods of time (eg. Hoitink, 2004; Deines, 1999; Holdaway et al., 1999). Such instruments can be deployed in the field and many are capable of transmitting data to shore or storing collected data that can be retrieved after recovery of the device. Acoustic devices that employ active sonar have the additional

benefit of measuring current velocities throughout the water column, which has been cited as a factor that influences turbidity in certain marine settings (Hointink, 2004).

This paper seeks to elucidate factors that affect turbidity at the experimental sites in Kaneohe Bay, Oahu. Through the use of data collected from a month long acoustic Doppler current profiler (ADCP) deployment in June 2005, connections between various physical forcing mechanisms will be examined as to their effect on suspended sediment load. Physical mechanisms that were examined include current velocities, tides, waves, and winds. In addition, a field experiment was performed to infer the reliability of ADCP estimates of backscatter to measured SPM concentrations.

Several studies have sought to characterize the marine environment of Kaneohe Bay, Oahu. The work of Moberly and Chamberlain (1964) classified the dominant wave regimes that affect Hawaiian waters. The most prevalent waves throughout the year are the Northeast Trade Waves, which are dominant between April and November. These are generated from strong tradewinds that originate from the northeast of the Hawaiian Islands. These waves are dominant over the times of the year when the ADCP deployments occurred and were shown by Shimada (1973) to exhibit strong wave energy. Tides in the bay are mixed-dominant, semi-diurnal. A paper by Bathen (1968) examined a number of Kaneohe Bay characteristics including currents that showed a dominant southwest flow over the deployment sites. However, the Bathen study ignores vertical current velocities.

Chapter 2: Methods

Fundamentals of the acoustic Doppler current profiler

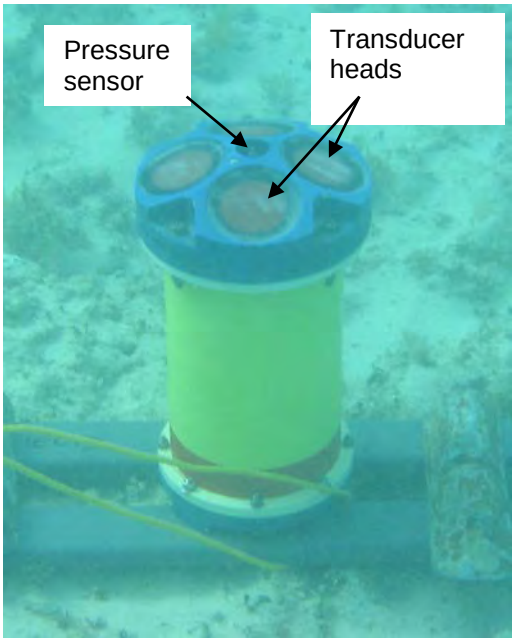

Figure 2.1: An ADCP deployed in the water with exterior components labeled

Acoustic Doppler current profilers use acoustic signals to obtain data about characteristics of the water column. As its name would suggest, an ADCP is able to determine the direction of target particles in the water column by utilizing the Doppler effect. The Doppler shift is the observed change in the frequency of a signal due to relative motion. For instance, for an observer facing a series of incoming waves, a certain number of waves, would pass by the observer over a given time interval. However, moving toward the source of the waves, the observed frequency would increase from that observed when stationary. This example illustrates the principle behind the Doppler shift, where the amount of shift recorded is proportional to the velocity of the observer.

The ADCP works by measuring a similar phenomenon known as Doppler time dilation and instead remains stationary while the particles in the water column are moving, opposite to the previous example. Transducers atop the ADCP (see Figure 2.1) transmit sound pulses (known as pings) into the water and then become receivers that "listen" for the returning signal. A series of echoes from a target scatterer will show a

change in the phase of the sound signal, a result of target movement between pulses. This change, known as propagation delay, combined with information about sound transmission through the water medium, can give you the velocity of particles at various depths in the water column (Gregg, 1996). The ADCP divides the water column into depth increments, or bins, and averages the data across an individual bin to produce a single variable's value. Due to the nature of the transducer, a blanking distance is associated with each data signal. The blanking distance is the range from the transducer face that is too close in proximity to allow enough time for the transducer to switch between transmitting and receiving the signal. The blanking distance of a signal will depend on the settings of the individual ADCP and on the frequency of ping transmission.

The RD Instruments Broadband Sentinel (see Figure 2.1) employed for data collection for this paper, houses four transducers mounted on the top of the ADCP instrument. These transducers work together to measure particle velocity in three-dimensions, with the additional constraint providing an error-check for the data. Through post-processing of the data, current velocities can be deconvolved into their north, east, and vertical components.

Fundamental to the operation of the ADCP is the assumption that the scatterers present in the water have low independent motility relative to water currents (Gregg, 1996). Thus, the propagation delay seen in the returned signal is due to the currents that move the particles responsible for reflecting the signal back to the transducers. The scatterers in the water column, off which the ADCP pings reflect, will be approximately the same size as the wavelength of the ping. For the 1228.8 kHz signal transmitted from

the ADCPs in this study, the dominant scatterer size will be on the order of 1.25 mm (Gregg 1996).

The ADCPs of the study were configured to emit 20 subpings every second, reducing the error that is inherent in an individual ping. Bin size was 0.05 m. According to RD Instrument calculations, the associated error in the measured current velocities was 0.33 cm/sec for each current datum.

In addition to information on current directions, the strength of the recorded acoustic signal provides an estimate of turbidity. This estimate known as echo intensity (EI) will be proportional to the amount of scatterers present in the water column. A top-mounted pressure sensor records data regarding tides and wave height.

Use of echo intensity to approximate turbidity

Echo intensity can be used as an analogue for turbidity. Simply put, more particles in the water will result in a stronger reflected signal and higher EI values. There are however, other factors that influence the EI signal. These include other attenuation factors such as absorption by particles and the water itself, signal spreading, and water temperature. These factors can be accounted for by the conversion of EI to acoustic backscatter using the equation (Deines, 1999):

$$S_V = C + 10\log_{10}((T_X + 273.16)\,R^2) - L_{DBM} - P_{DBW} + 2\alpha R + K_C\,(E - E_r)$$

where S_V is the backscattering strength (dB re $(4\pi m)^{-1}$), C is a constant that accounts for a number of ADCP characteristics, measurable by the user, T_X is the temperature of the transducer (ºC), R is the slant range to the scatterers (m), L_{DBM} is the transmit pulse

length ($10\log_{10}(m)$), P_{DBW} is the transmit power ($10\log_{10}(W)$), α is the absorption coefficient of water (dB/m), K_C is the response of receivers to input strength, E is the measured EI, and E_r is the reference EI level.

Echo intensity was used as an analogue for turbidity as opposed to acoustic backscatter (S_V) because many of the comparisons that were made between EI used a depth-averaged signal. Although a number of variables are accounted for in S_V calculations, the primary purpose of this conversion is to account for a loss of signal due to propagation away from the instrument. A depth sample interval (known as a bin) will be expected to return a stronger signal to the transducer than a bin some distance away, for a homogeneous water column. Averaging across all depths of the water column eliminates the majority of variation due to depth and thus depth-averaged echo intensity (DAEI) was deemed sufficient for the majority of project analysis. However, it should be noted that there is bias in the DAEI data that give higher weights to the values near the bottom. The higher SPM concentrations near the bottom are subject to less attenuation of the acoustic signal and will be overestimated by echo intensity.

Water samples for echo intensity calibration experiment

An attempt to calibrate EI data was made in order to gauge transport rates, confirm assumptions regarding scatterer size and characterize the response of EI to changes in SPM concentrations. Water samples were taken using a Niskin sampling bottle at 10-minute intervals, downcurrent of an ADCP positioned on the reef bottom. Samples were then returned to the lab for filtration and drying. Echo intensity values, as

measured from an ADCP were compared to SPM concentration data. Further details are presented in the *Observations* section under *Deployment 3*.

Low-pass filtering of data

Due to the complex nature of EI response to an array of marine forcing mechanisms across a wide range of temporal frequencies, data filtering was used to isolate individual responses to forcing at low frequencies and discern long-term trends. The filter used for this procedure was a weighted-mean (Butterworth) filter, which weights values according to the their proximity to the individual datum and averages values at the filter order (Mathworks, 2006). The time length of the filter order that was chosen for analysis varied according to the individual factor of interest. For instance, waves were filtered on periods of 24-hours to remove the variations due to tides.

Chapter 3: Observations

The ADCP deployments that produced the data for this study were located in the waters of Kaneohe Bay on the eastern shore of the island of Oahu. Kaneohe Bay stretches 12.72 km along the coast and has a maximum width of 4.26 km, orthogonal to the coast (Bathen, 1968). A barrier reef extends along the length of the bay, limiting flow into the bay. Trade winds, originating from the northeast, are the dominant wind regime

Data from three separate ADCP deployments were used in the analysis of turbidity and its determinant factors. ADCPs were positioned atop the reef flat, in close proximity to Kapapa Island (see Figure 3.1).

Figure 3.1: Location of ADCP deployment sites (modified from Google Earth)

Sampling frequency and deployment length varied between each of the deployments and are described in the following subsections.

Deployment 1: Data from Deployment 1 were obtained from Geno Pawlak of the Ocean and Resources Engineering Department at the University of Hawaii. Deployment 1 involved a single ADCP, located at 21.4705º N and 157.7987º W, hereafter referred to as Site 0. Deployment 1 lasted for eight days, from Aug. 21 to Aug. 29, 2003. Data were obtained every hour, with each datum representing the averaged value over this one-hour period. Due to the relatively short deployment of the ADCP, data taken at Site 0 were used primarily in this paper to confirm the relationships that were identified in Deployment 2, particularly those at Site 1.

Deployment 2: The data that constitute Deployment 2 were obtained from Jim Falter and Marlin Atkinson (Hawaii Institute of Marine Biology (HIMB)) and Ryan Lowe (Stanford University). Deployment 2 involved three ADCPs, spaced approximately 950m apart and oriented in a line, parallel to the shore and reef flat. The ADCPs, hereafter referred to as Sites 1, 2, and 3, were located at 21.4716º N, 157.7986º W; 21.4786º N, 157.8073º W; and 21.4825º N, 157.8135º W, respectively. Site 1, the furthest south of the Deployment 2 ADCPs, was located in close proximity to Site 0, approximately 120 m to the north of Site 0.

ADCP data from Deployment 2 represent a month-long time series from June 7 to July 8 of 2005. Due to battery constraints during the deployment, the instruments were cycled on and off (burst sampled) every 15 minutes. Thus, datum points represent the averaged values for every other 15-minute period.

Deployment 3: Deployment 3 involved a single ADCP that collected in conjunction with water column sampling. The ADCP used in deployment 3 was located at 21.4625 ºN, 157.8050 ºW, hereafter referred to as Site 4. The Site 4 deployment lasted 2 1/3 hours, from 14:20 to 16:40 on August 20, 2006. Data were sampled every second.

Water samples were taken using a 2.3L Niskin bottle. Samples were taken at approximately 2 m depth every 10 minutes. Due to inconsistencies in the lowering of the Niskin bottle (see *Discussion*), the bottle was allowed to clear for 5 seconds after bottom contact, before collection of the water sample. Samples were returned to the lab, where they were individually vacuum filtered through a 0.45µm glass fiber filter. The volume of each sample was taken prior to filtering using a 500 mL graduated cylinder. Filters were then placed in a drying oven for 48 hours. Filters were placed atop a 0.1mg mass balance using tweezers. Suspended particulate matter concentration was taken as the mass difference of the filter before and after filtering of the sample, divided by the volume of each sample (mg/L). Filters were weighed 3 times, to minimize precision error by the mass balance.

Ancillary Data: Wind, Solar Radiance and Offshore Waves

In addition to the data collected from the ADCP deployments, ancillary data were also obtained for inclusion in data analysis (see Figure 3.2). Wind and solar radiance data were obtained from the HIMB at Mokuoloe (Coconut) Island and offshore wave data from the Mokapu buoy, operated by the Coastal Wave Group at the University of Hawaii at Manoa.

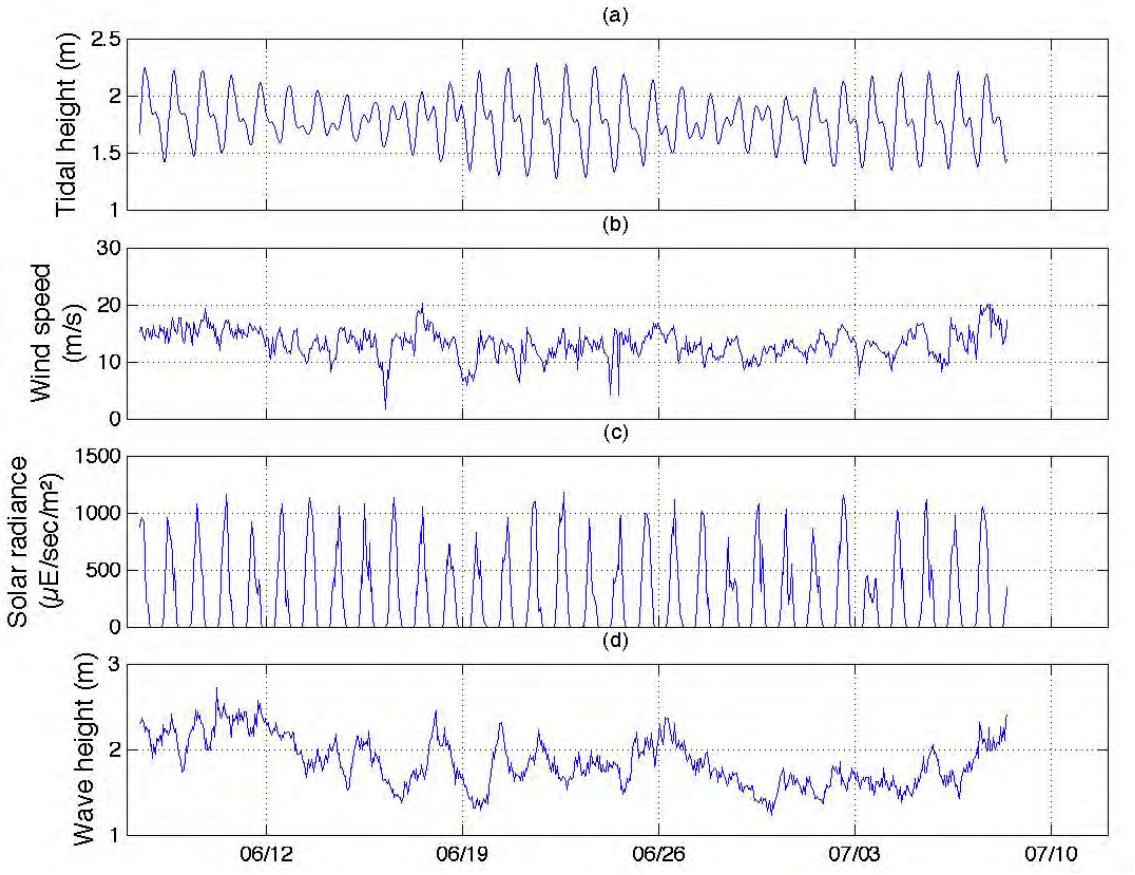

Figure 3.2: Ancillary data for Deployment 2: (a) tidal height, (b) wind speed, (c) solar radiance, and (d) offshore wave height. Tidal height was taken from Site 1 data, which were sufficient to represent the tidal variation across all Deployment 2 sites

The HIMB weather observatory at Mokuoloe Island provided hourly data wind and solar radiance data in Kaneohe Bay. Average wind speed over the Deployment 2 was approximately 6 m/sec. Winds were constantly blowing from the NE except for 6 hour periods of northerly winds observed on 6/15/05 and 6/28/05. These data were consistent with typical summer conditions of Kaneohe Bay (Shimada, 1973). The mean solar radiance during daylight hours was 476.2 $\mu E/sec/m^2$ and on average reached its maximum value at the 13:00 sample time.

Wave data from the Coastal Wave Group Mokapu buoy served as a measure of offshore wave heights. Wave height varied from 1.23 m to 2.72 m with a mean of 1.87 m.

Chapter 4: Results

Echo intensity variation across Deployment 2

Echo intensity varied significantly across the different sites. As stated previously, due to its significantly shorter deployment time and close proximity to Site 1, the Site 0 ADCP data primarily served to verify the relationships that were observed at Site 1. Figure 4.1 shows the EI at Sites 1-3 for the month-long deployment. The color shaded plot illustrates the EI at each depth across the time series, while the line plot at each site represents the depth-averaged echo intensity (DAEI).

The largest DAEI values occurred at Site 1 while Site 3 exhibits the smallest DAEI values.

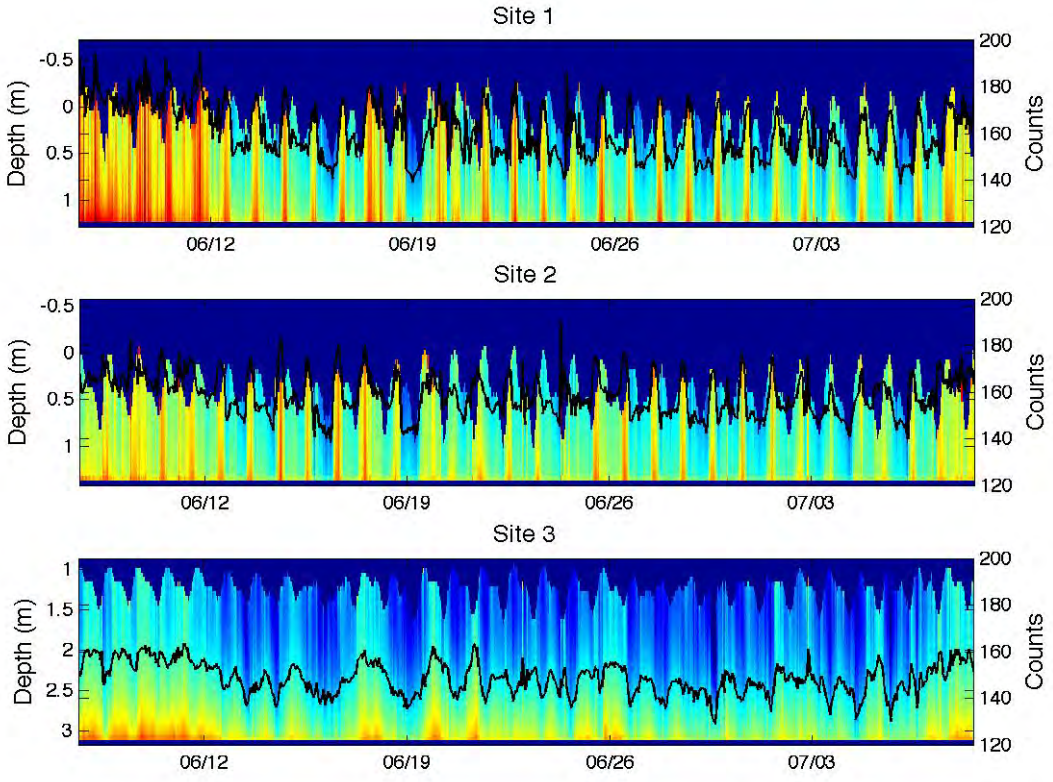

Figure 4.1: Echo intensity time series for Deployment 2 with depth-averaged overlay (—)

Relationship between wave height and echo intensity

Low frequency variations in EI show a strong relationship with wave height. The wave heights themselves, defined as the highest one-third of waves within a sample period (significant wave height), show a strong correlation to tidal range (i.e. water depth increases, waves propagate further inshore before energy is dissipated through breaking). To account for this, a 24-hour, low-pass filter was applied to the significant wave height signal in order to remove the tidal influence that occurs over this period. Echo intensity, also subjected to a 24-hour low-pass filter, was then compared to the filtered wave signal (Figure 4.2).

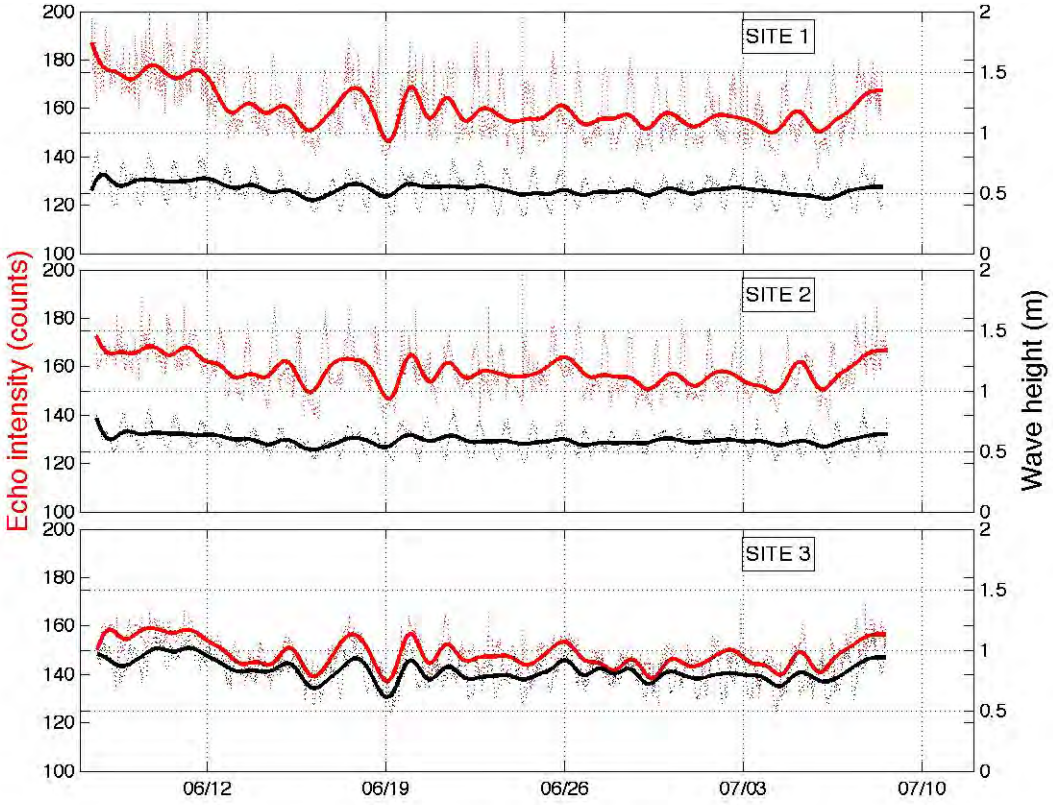

Figure 4.2: Echo intensity and wave height comparison. 2 ½ day low-pass filtered results for DAEI (—) and wave height (—)

In addition to the tidal dependence found in the significant wave signal, winds also act to drive waves (Appendix 1). This wind-wave relationship is most pronounced at Site 3.

An important concept in understanding the influence of waves at different study sites is the depth at which waves in Kaneohe Bay are expected to break. Komar and Gaughan (1972) obtained a formula for estimating the breaking depth of waves as:

$$H_b / H_\infty = (0.563 / (H_\infty / L_\infty)^{1/5}$$

Where H_b is the breaker height, H_∞ is the offshore wave height, and L_∞ is the offshore wavelength, obtained using the equation:

$$L_\infty = gT^2 / 2\pi$$

where g is the gravitational constant and T is the offshore wave period.

Offshore wave data from the Mokapu buoy show a mean T = 7.53 sec and a mean H_∞ = 1.87 m, yielding a value for H_b of 2.27 m breaker height. H_b can be related to breaking depth by the equation (Komar 1998):

$$\gamma_b = H_b / h_b$$

where γ_b is the critical breaking wave ratio and h_b is the water breaking depth. Typically, γ_b = 0.78 in nearshore environments, which yields a breaking depth of 2.91 m, approximated to 3 m.

The 3 m estimated breaking depth falls between the depths seen at Sites 0-2 (<2 m) and that found at Site 3 (3.5 m). Sites 0-2 are in depths shallower than the 3 m wave-break isobath, while Site 3 is located outside of the breaking zone, where waves are expected to maintain a larger fraction of their energy (see Figure 4.3).

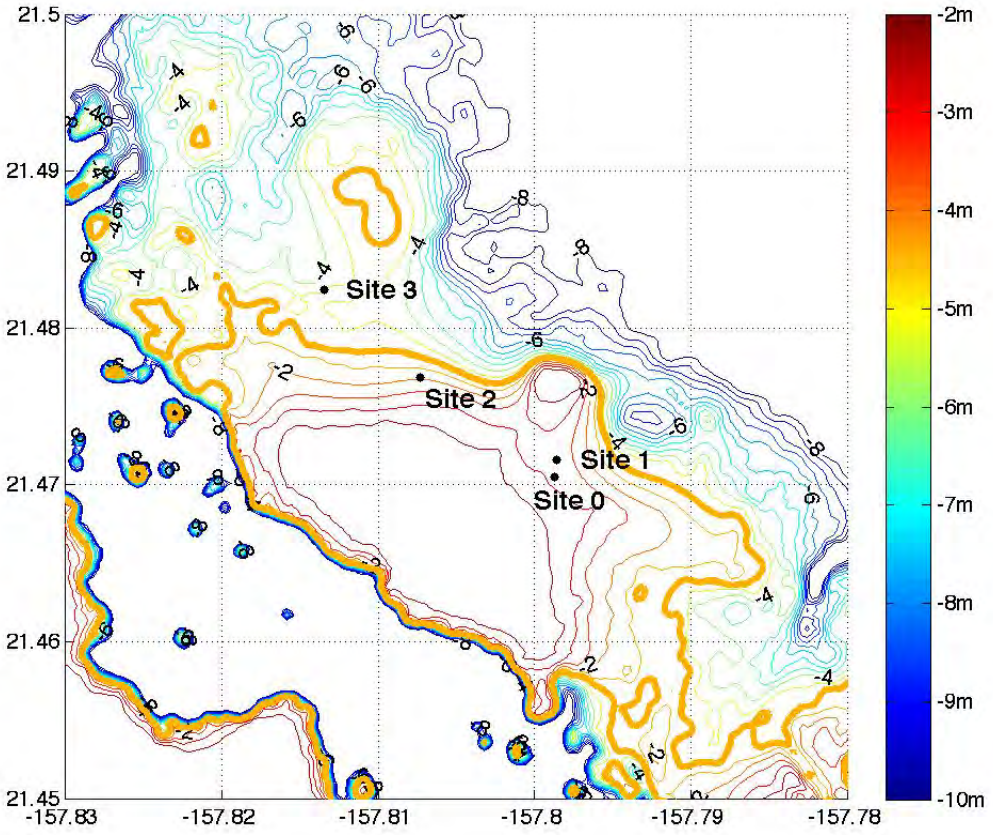

Figure 4.3: Bathymetry at Sites 0-4 with 0.5m isobaths. Bold line (—) represents 3 m isobath, corresponding to the estimated breaking depth of waves for Kaneohe Bay

Relationship between current velocities and echo intensity

There is a covariant relationship between current speed and EI. This relationship is shown in Figures 4.4 - 4.6, with current velocities plotted for individual ADCP sites. The location of each point in the figures indicates speed, taken as the distance to the origin, and direction, relative to its respective ADCP site. The color of each datum point indicates the DAEI value that was measured over the same time sample.

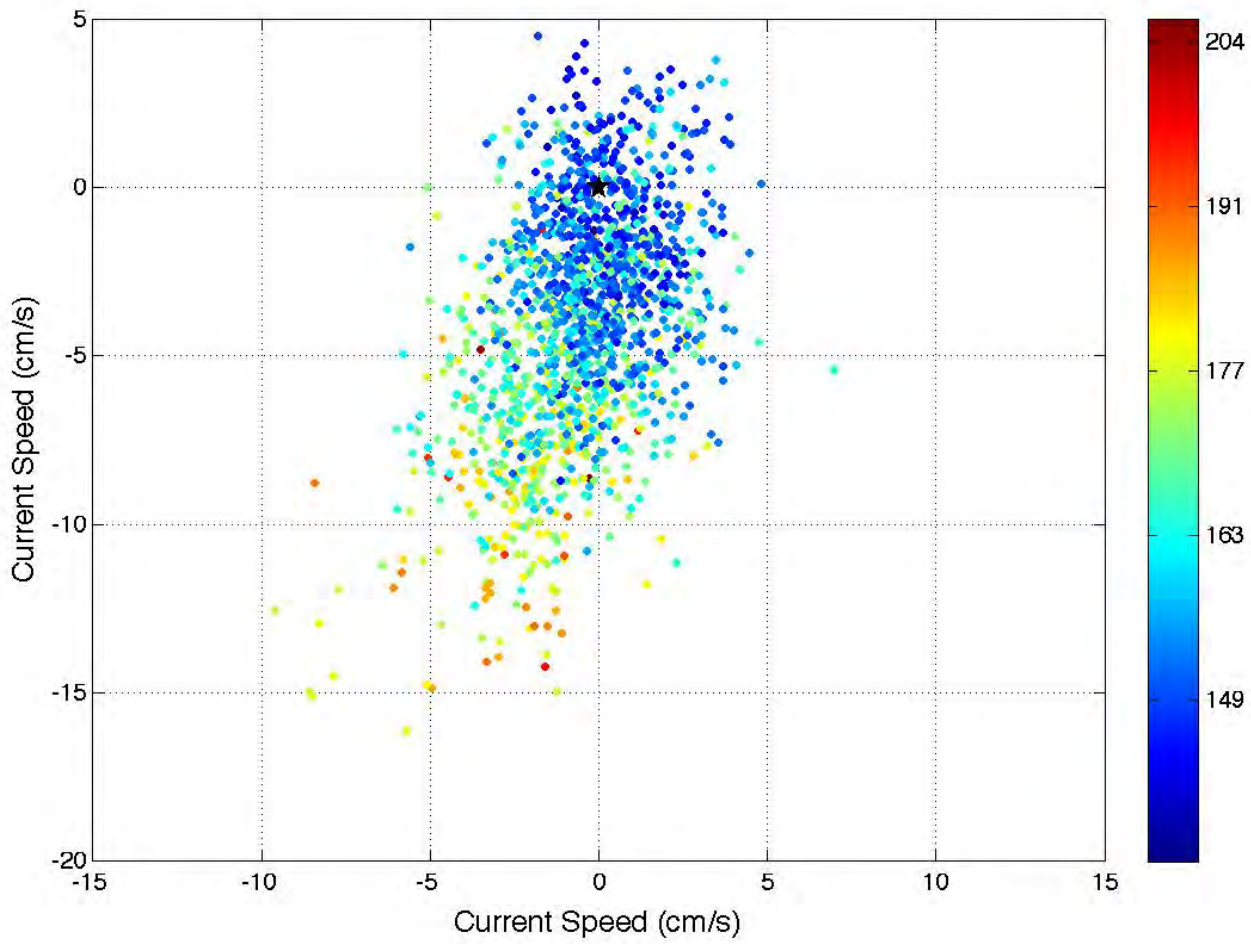

Figure 4.4: Current velocities for Site 1. Each data point corresponds to the speed and direction at each sampled time, relative to the origin. Echo intensity is plotted as each point's color index, coinciding at its respective time

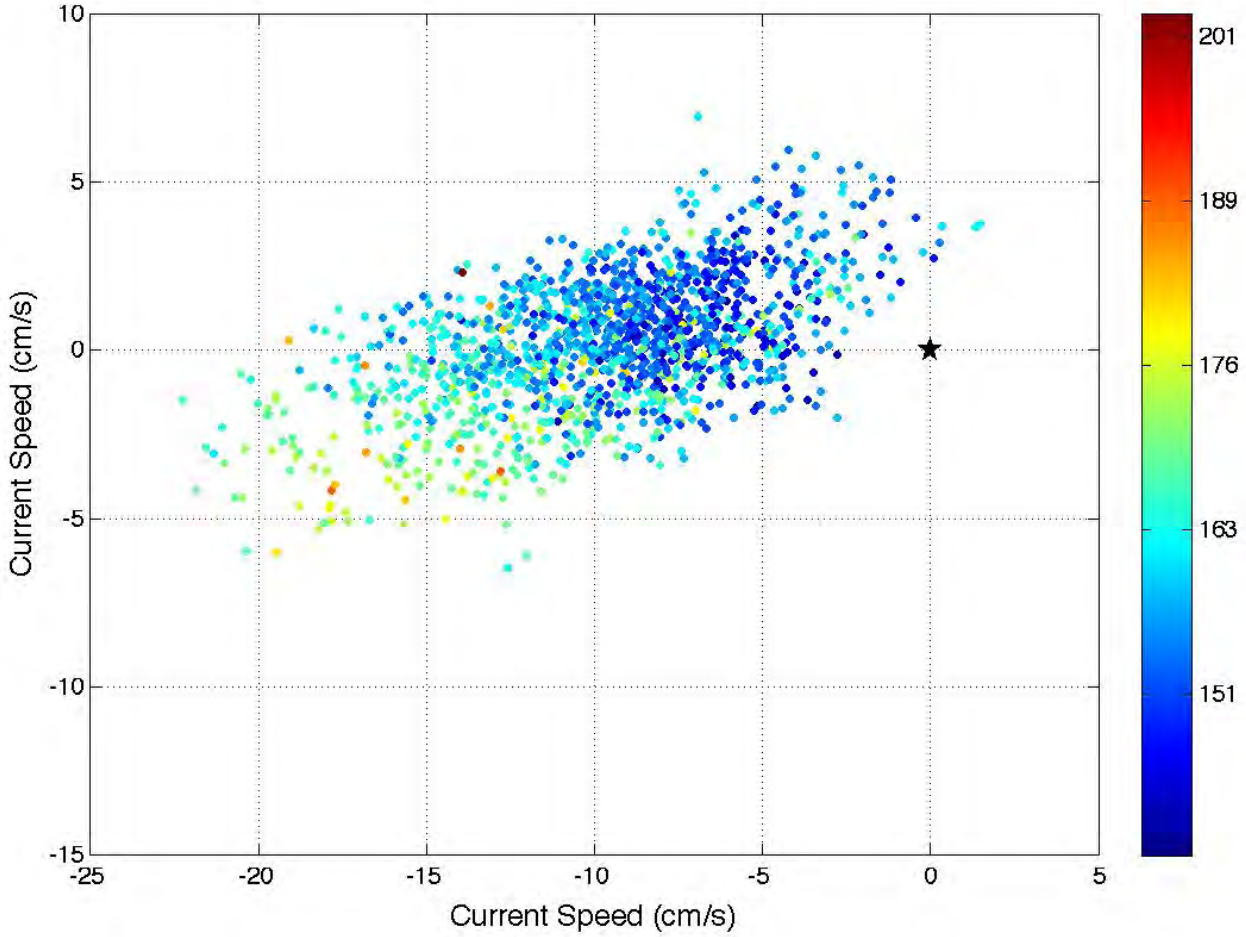

Figure 4.5: Current velocities for Site 2. Each data point corresponds to the speed and direction at each sampled time, relative to the origin. Echo intensity is plotted as each point's color index, coinciding at its respective time

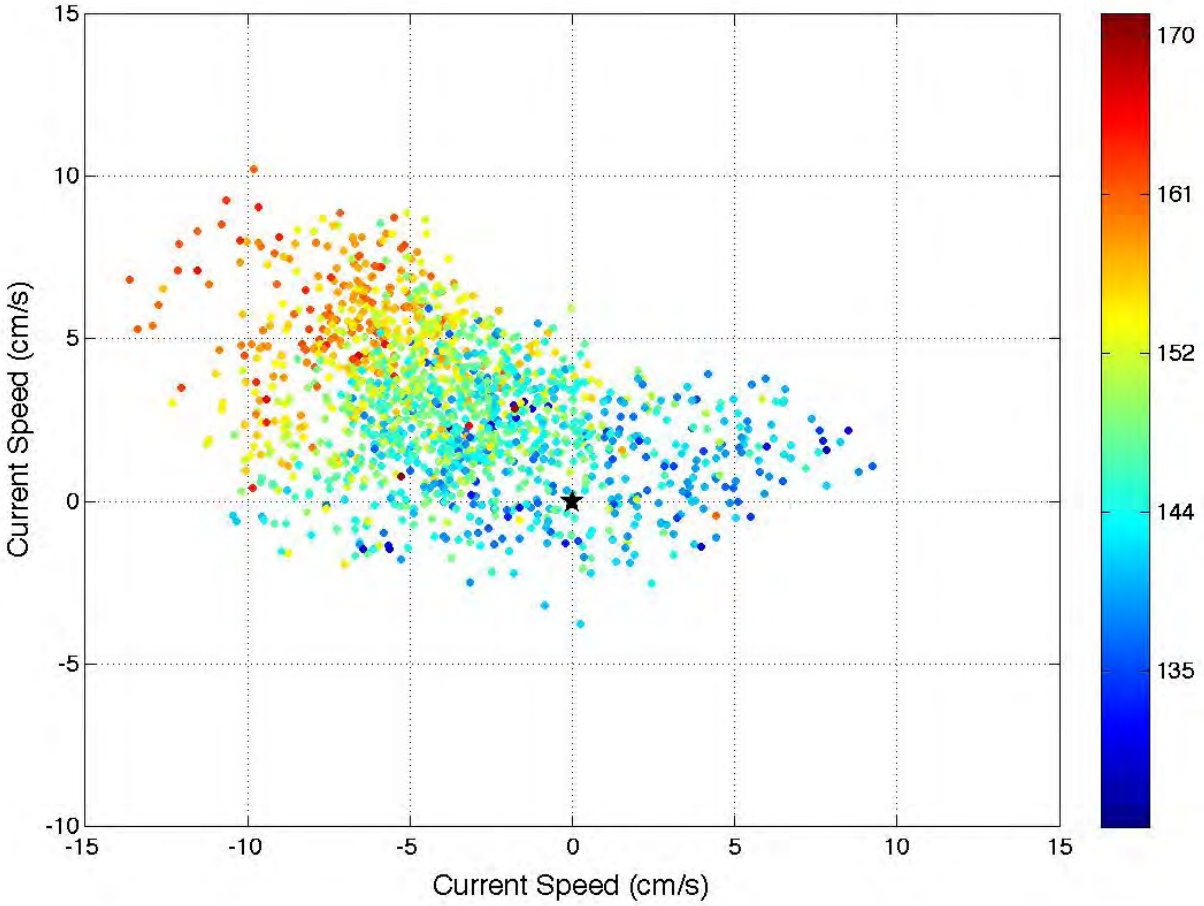

Figure 4.6: Current velocities for Site 3. Each data point corresponds to the speed and direction at each sampled time, relative to the origin. Echo intensity is plotted as each point's color index, coinciding at its respective time

All sites exhibit little cross-shore oscillation. Instead, currents maintain a consistent flow direction, varying primarily in speed. These data are in general agreement with the findings of Bathen (1968). Site 3 shows the greatest variation in current direction. Despite this, the majority of high current speeds at Site 3 are directed to the northwest and correspond the highest DAEI values at the site.

Relationship between time of day and echo intensity

Although the original intent of this paper was to identify the physical forces that influenced suspended solid concentrations, visual analysis suggested that EI peaked on a diurnal cycle. Figure 4.7 shows the daily distribution of DAEI values from the entire data series at each site, plotted according to its respective time of day in half hour intervals.

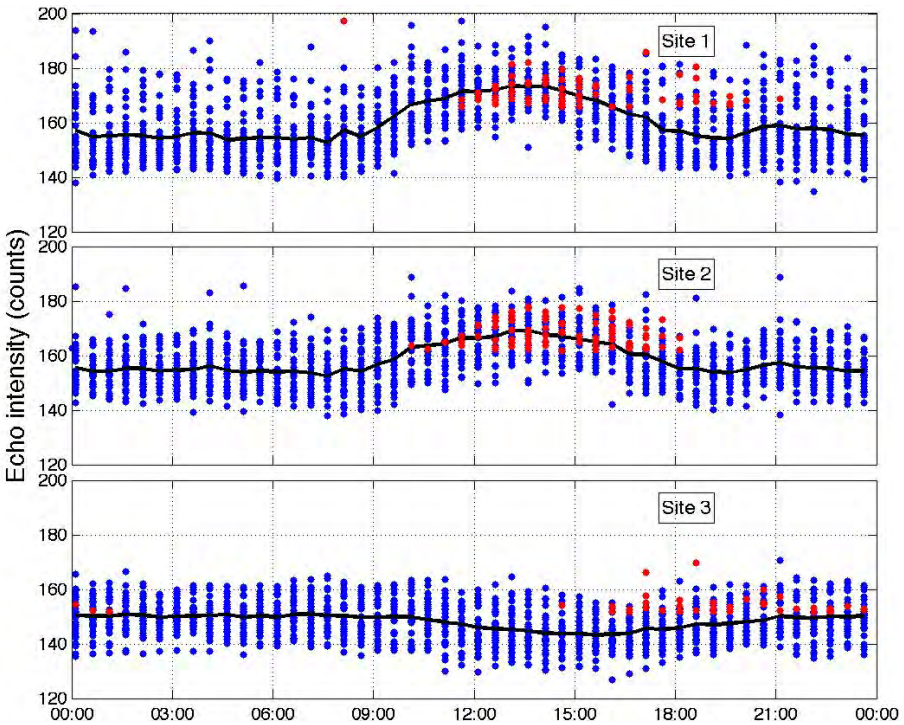

Figure 4.7: Daily variation in DAEI, grouped by time of day, with low-velocity, high DAEI data (red)

Sites 1 and 2 exhibit a clear peak in EI values in the early afternoon. The time series for each plot is characterized by higher EI values at approximately 13:30 and a lack of the lower EI values that are present at other times of the day. The afternoon peak in the DAEI count is also present in data from Site 0 (see Appendix 2).

At Site 3, the relationship observed at Sites 1 and 2, between the solar radiance and DAEI, is absent. Instead, there appears to be the opposite relationship. Plotted as a function of the time of day, DAEI data from Site 3 show a daily minimum at 15:00, although this minimum is not as pronounced as the maximums at Sites 1 and 2.

The current velocity plots for all three sites (Figures 4.4 – 4.6) contain points that indicate high DAEI that are associated with low current velocities. A data screen was used to identify points that fell within the lowest 33-percentile of current velocities and the highest 33-percentile DAEI. This yielded n = 69 out of 1488 for Site 1, n = 90 out of 1488 for Site 2, and n = 43 out of 1483 for Site 3. The time index for each point was plotted on the graph of DAEI variation as a function of time (see Figure 4.7, red points). At sites 1 and 2, these low-velocity points occurred in the afternoon. At Site 1, outlier points that occurred in the late afternoon corresponded to DAEI values from early in the time series, prior to 6/12/05, where high DAEI values were observed (see Figure 4.1).

Figure 4.8 shows the DAEI signal at Sites 1, 2, and 3 averaged across each hour of the day. Peak DAEI at Sites 1 and 2 appears to correspond to the peak solar radiance measured at Mokuoloe Island over the same time period.

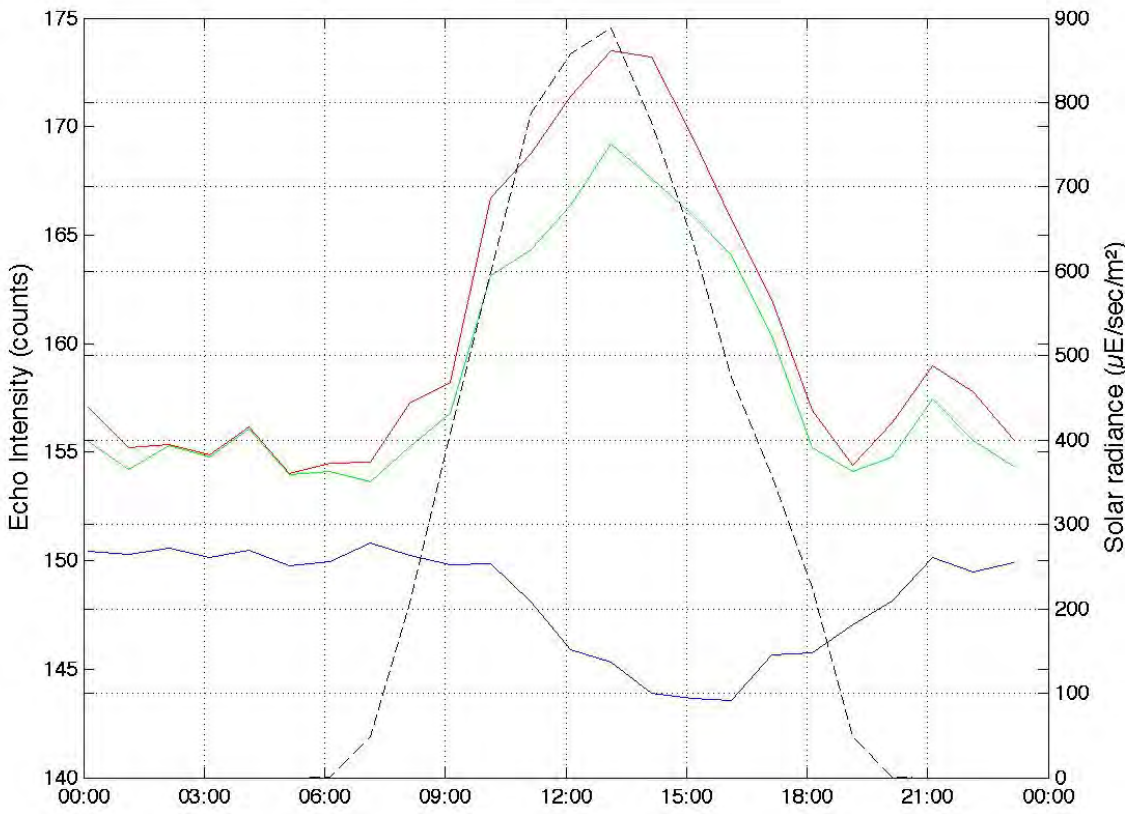

Figure 4.8: Average daily value of Site 1 DAEI (—), Site 2 DAEI (—), Site 3 DAEI (—), and solar radiance (- -)

The radiance dependence observed at Sites 1 and 2 appears to not be due to vertical migration of organisms. Covariance analysis was performed between the DAEI data and solar radiance data. Results from the covariance analysis showed that there was little change in the lag exhibited between the daylight function peak and EI values (Figure 4.9) at increasing distance from the ADCP.

Cross covariance analysis showed that EI lagged peak solar radiance by approximately one hour. Vertical migration of organisms would exhibit an increasing lag at distances further from the ADCP. The lack of a change in the covariance functions across different depths suggest that vertical migrations of organisms does not occur or

that it occurs on a temporal scale of less than a half hour. Although there are changes in the cross covariance values at Site 2, the lag does not change across depth bins.

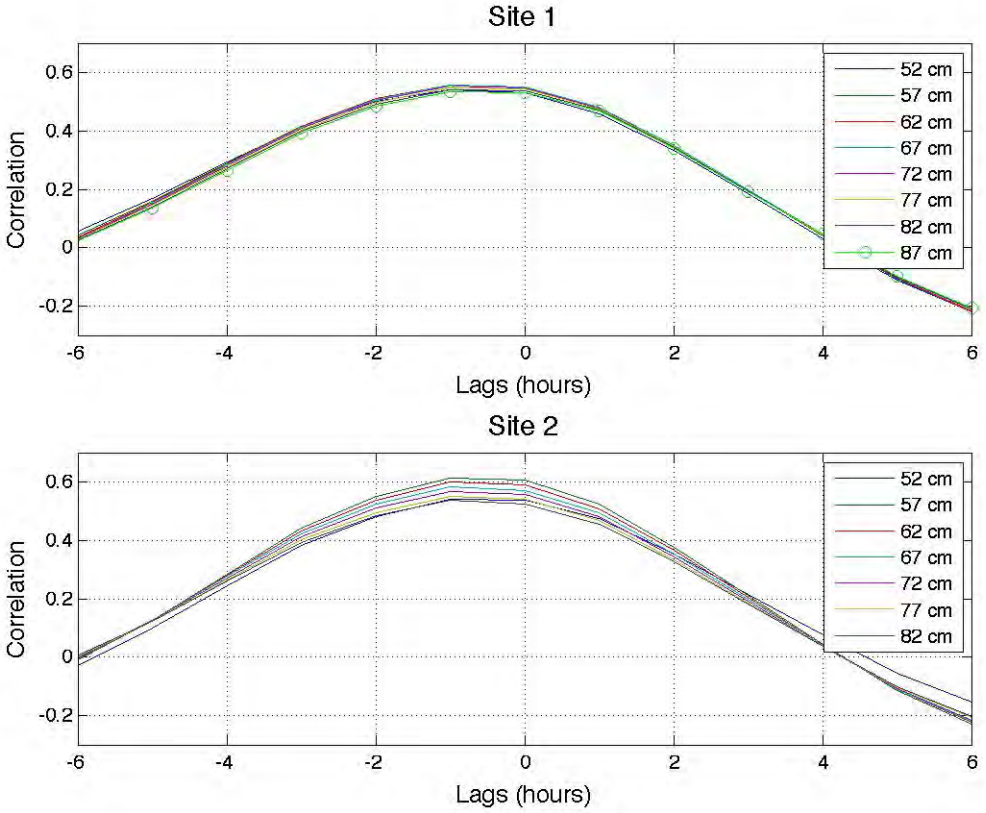

Figure 4.9: Covariance between solar radiance and EI, by distance from bottom

Relationship between vertical currents and echo intensity

A very strong covariant relationship can be seen between DAEI and vertical current speed at Sites 1 and 2 (see Figure 4.10). Similar to the solar radiance relationship described earlier, however, this relationship is noticeably absent at Site 3. In addition, Site 3 exhibits downward currents throughout nearly the entire time series.

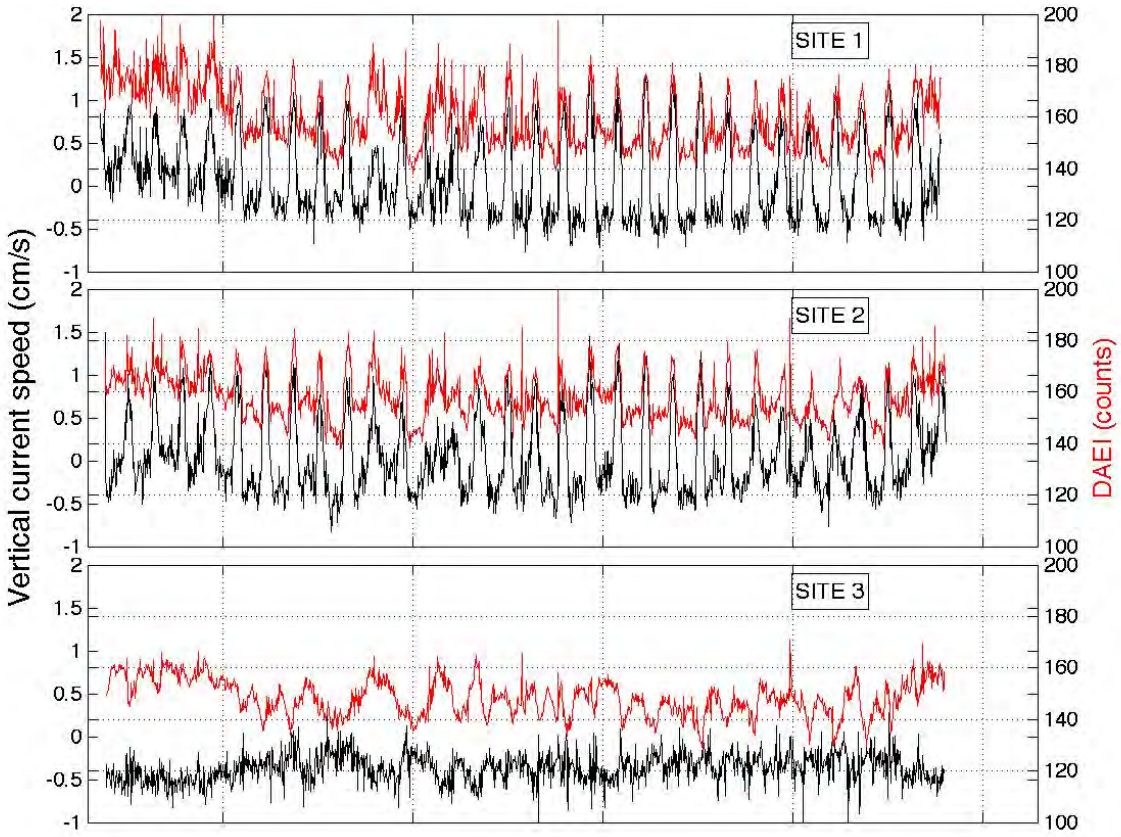

Figure 4.10: Depth-averaged vertical current speed (—) and DAEI (—) comparison

The covariant relationship at Sites 1 and 2 can also be seen through covariance analysis of the DAEI and vertical current speed data (Figure 4.11). Sites 1 and 2 show a strong and immediate response in DAEI to changes in current speed. Such a response does not occur at Site 3.

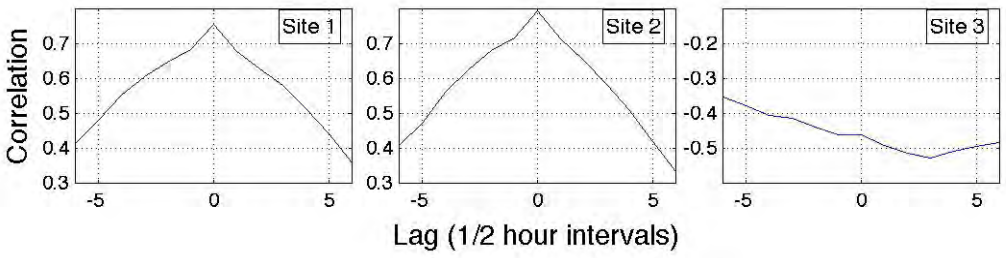

Figure 4.11: Covariance between vertical current speed and DAEI

In order to further evaluate the relationship between vertical currents and DAEI, Site 0 data were examined. Site 0 exhibited no substantial relationship between DAEI and vertical current speed (see Figure 4.12). This lack of response may be due to a lack of a dominant horizontal current direction at Site 0 (see Appendix 3) or the relatively small dataset from hourly data sampling over the one-week deployment.

It should be noted that the vertical current speeds measured at all sites are potentially subject to significant error. Although an averaging of pings was performed to increase precision, error values for these averaging intervals, obtained through RD Instrument calculations, were shown to be approximately 0.33cm/sec. This error is significant relative to the range of observed vertical current speeds.

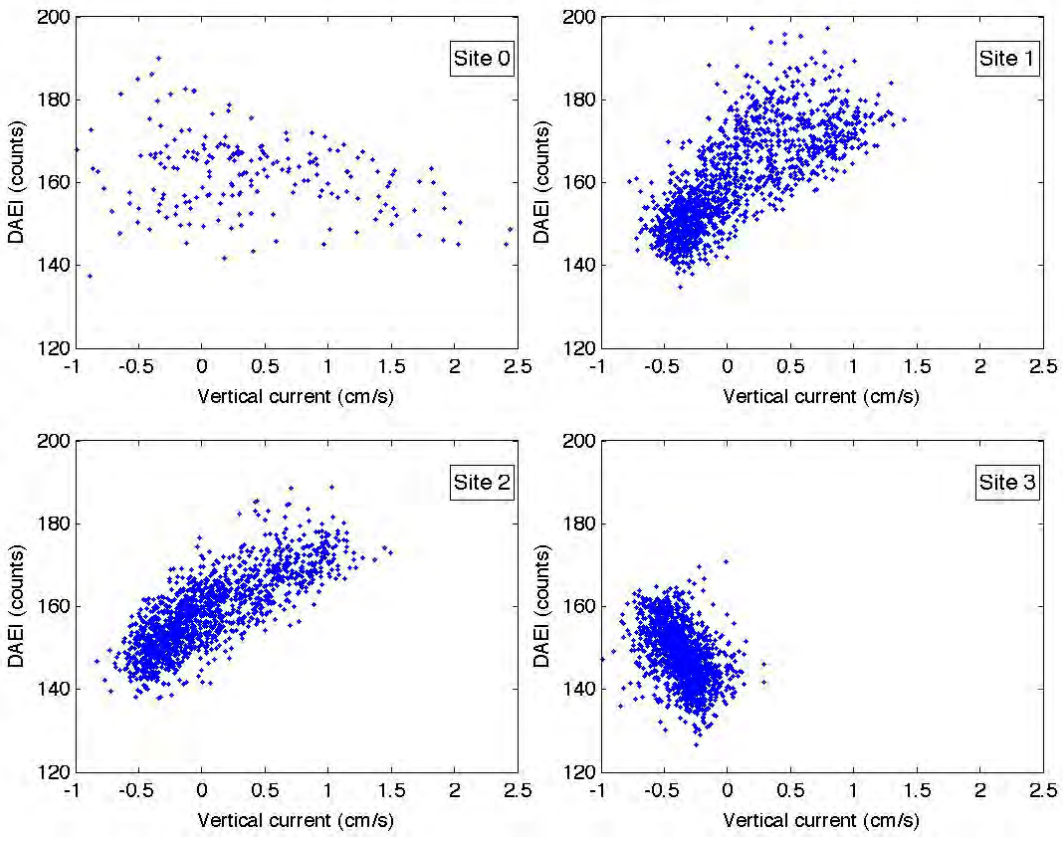

Figure 4.12: Depth-averaged vertical current velocity vs. DAEI, Sites 0-3

Calibration experiment results, Deployment 3

In an attempt to correct for the spatial differences between the ADCP and water sample site, the EI data used in the comparison to SPM concentration data were one minute average of data collected two minutes prior to each water sample. This was based on an assumption that a change in SPM concentration at the ADCP would take approximately 1.45 minutes to travel the 20 m distance to the vessel along a southeast current with an average velocity of 23 cm/sec, as sampled by the ADCP.

The results from the calibration experiment are shown in Figure 4.10. Figure 4.13a shows the ADCP data, averaged over the 2 minutes prior to the time of collection of the water sample. The line plot represents the DAEI over this

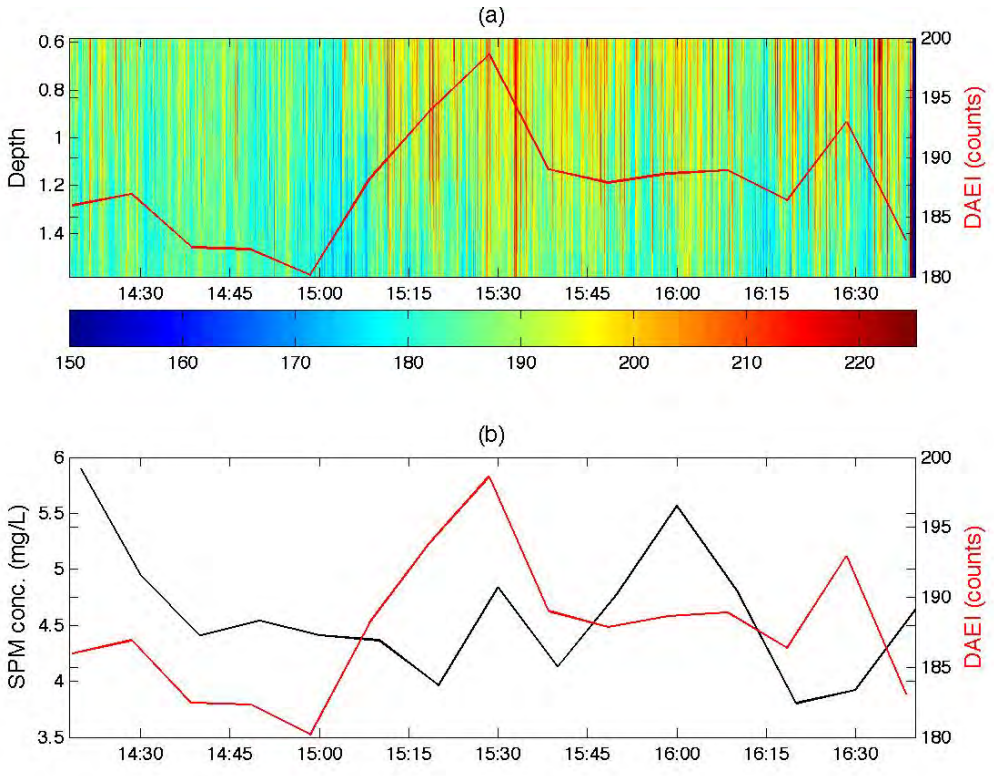

Figure 4.13: (a) Raw DAEI data, with sample time of 1 sec, overlaid with 1-min averaged DAEI (—) (b) Comparison of results from calibration experiment relating DAEI (—) to SPM concentration data (—)

same period. The lower plot (Figure 4.13b) shows the mass of the SPM concentrations that were measured by sampling of the water column with a DAEI data overlay.

The DAEI signal produced from the ADCP did not match the observed SPM concentration variance. However, as Figure 4.13a illustrates, there is a very high variability associated with DAEI. Used as an analogue for SPM concentrations, the DAEI data would suggest a high variability is also associated with each water sample. Although steps were taken in the experiment to reduce error, the small SPM concentration values, in conjunction with the highly variable nature of the sampling environment, makes it difficult to draw any conclusions relating DAEI to SPM concentrations from the data that was collected.

Figure 4.14 shows DAEI and SPM concentrations plotted against one another. Vertical error bars represent the standard deviation of the weighing procedure, taken from each filter being weighed three times. The horizontal error bars represent the standard deviation of the DAEI signal, taken across all depths that were averaged to produce each DAEI datum.

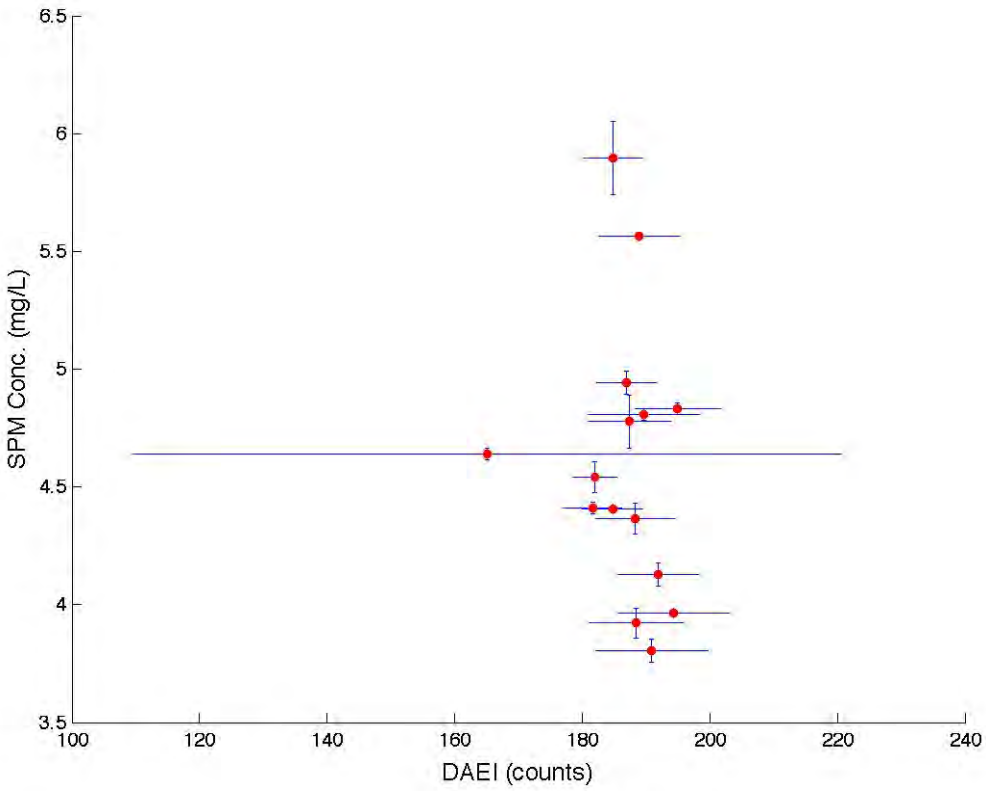

Figure 4.14: Relationship between DAEI and SPM concentration, Deployment 3 experiment

Chapter 6: Discussion

Suspended particulate matter concentrations appear to be influenced by a number of physical forces at the Kaneohe Bay deployment sites. Although these forcing mechanisms affect SPM concentrations (as approximated by DAEI) in a complex manner, differences in the temporal frequencies at which these physical mechanisms change can be used to somewhat isolate the individual effect that each has on DAEI.

Currents were shown to influence DAEI on periods of 24 hours or less. Sites 1-3 show a generally covariant relationship between horizontal current speed and DAEI. Sites 1 and 2 were shown to be strongly influenced by vertical currents, which had a very strong influence on DAEI. However, this relationship was not seen in the data from Site 3 of Deployment 2 or the data from Site 0 of Deployment 1, the latter of which was positioned in close proximity to Site 1, at a different time.

A diurnal cycle in DAEI was also observed at Sites 1 and 2, with a peak in DAEI occurring in the afternoon. This peak slightly lagged the peak in solar radiance by approximately one hour and was observed at Site 0, as well. An afternoon diurnal peak might suggest a biological source of SPM.

Although strong correlations at Sites 1 and 2 were shown in the data, the contradictory DAEI response to vertical current speeds at Site 0 remains unresolved. Further exacerbating attempts to isolate the solar radiance and vertical current influence was a diurnal cycle observed in the vertical current velocity data. This trend can be seen in Figure 5.1, which groups depth-averaged vertical currents according to their occurrence during the day. Horizontal currents exhibit neither a clear diurnal cycle (see Appendix 4) nor any discernable relationship to vertical current velocities.

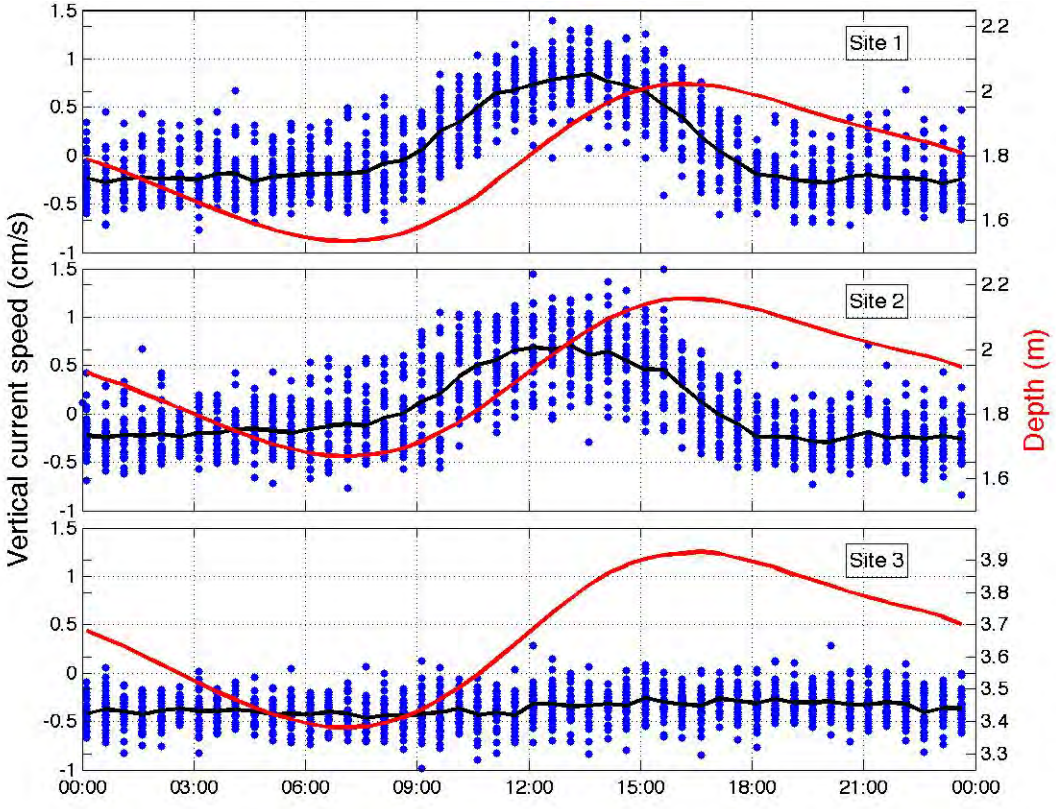

Figure 5.1: Daily variation in depth-averaged vertical current velocities, grouped by time of day, average daily current velocity (—), and average daily depth variation (—)

A diel maximum, nearly identical to the DAEI maximum, can be observed in the early afternoon at approximately 13:00. It is likely that vertical currents were being driven by the incoming tide (shown as increasing depth in Figure 5.1) that on average, occurred more often in the afternoon during the Deployment 2 period. The peak in vertical currents appears to coincide with the maximum change in depth. Incoming tides are generally shown to be associated with onshore water movement. These onshore currents move up the sloped reef, resulting in vertical velocity component.

The afternoon increase in DAEI at Sites 0-2 may also be attributable to biological organisms. This hypothesis would suggest that diurnal migration of zooplankton might be responsible for the afternoon peak. Additional data from Kaneohe Bay that serve to support this contention, however, could not be found. The lack of a change in the covariance lag between solar radiance and EI would suggest that vertical migration does not occur. It is still possible however, that vertical migration of zooplankton occurs on a time scale shorter than a half hour, especially when the shallow water depths of the sites are taken into consideration.

Of significance to the vertical migration theory are unpublished chlorophyll data from the Coral Reef Instrumented Monitoring Platform (CRIMP) buoy located at Lilipuna Channel in south Kaneohe Bay (De Carlo et al., unpublished). A data series, taken over a 5-day long deployment showed an expected diel cycle of photosynthesis, illustrated by a peak in dissolved oxygen (DO) saturation. This DO maximum appears to coincide with, or slightly lag the peak in solar radiation, as seen earlier in the DAEI time series. However, chlorophyll levels do not show this same diurnal variation (see Appendix 4). This would suggest that chlorophyll-producing organisms remain in the water column after daylight hours rather than dispersing, as seen in the DAEI data.

There are not enough data to determine the composition of the SPM that are responsible for the EI signals measured by the ADCP. Although estimates of particle size can be made based on the wavelength of the ADCP acoustic pulses (on the order of 1.25mm), chlorophyll sensors or sediment traps were not deployed in conjunction with the ADCPs.

The author poses two possible explanations for the diel patterns in the DAEI time series. First, vertical current velocities are the primary forcing that dictates DAEI change and thus turbidity. This is likely an influencing factor at Sites 1 and 2, as shown in the strong and immediate response observed through the covariance analysis (Figure 4.11). It then is merely coincidental that the peak occurs in the afternoon, the time when incoming tides tend to occur over the course of Deployment. 2. In longer studies, this afternoon tidal bias would be expected to disappear and vertical currents would be expected to exhibit a covariant relationship with tidal height. The lack of response to vertical currents at Site 0 may be due to its location inland of Site 1, although the actual effect that this spatial difference could have on vertical currents remains unresolved. The more likely explanation is the difference in deployment length. Deployment 0 lasted only one week and thus experienced fewer variations in conditions than Sites 1-3. The one-week sample period was probably too short for a strong signal relationship to be manifested in the data. Secondly, it is possible that diurnal vertical migration occurs at Sites 0-2. This process might occur on a smaller time scale than that measured by the ADCP and would thus not show up in the EI depth analysis. It does not appear that the diel variations of Deployment 2 are caused by physical forces that act on a diurnal cycle (see Appendix 3).

The lack of a diel variation at Site 3 and overall different behavior also remain unresolved, considering the close proximity of the site to the other ADCP deployments. One possible explanation for the lack of a diurnal DAEI signal is the bottom type at Site 3, which is located atop a sandy bottom, as opposed to the reef environment of Sites 0-2. A sandy bottom may exhibit less resuspension of particulate matter than a reef

environment. Site 3 is also located in approximately 3.5 m water depth, nearly double that found at the other sites.

The influence of waves on EI shows a straightforward relationship across all sites at low frequencies. This relationship is highlighted by strong correlations and little lag between significant wave height and DAEI, once the short temporal variations of less than 2-days are removed. This may be caused by the stirring of bottom solids in the surf zone, which are then mixed through the water column. High SPM concentrations from the surf zone would then be carried inshore by the prevailing currents, which are directed toward Sites 1 and 2. This process may partially explain the higher DAEI data found at Sites 1 and 2.

The inability of the calibration experiment to produce usable results was likely due to a number of factors. The first was the conditions at the site of the experiment. High winds and surf prevented the experiment from taking place closer to Kapapa Island and the other sites. The rough marine conditions also hindered the experiment in a number of ways. The strong prevailing winds and currents caused the sampling vessel to drift considerably about the anchor point. Strong currents resulted in inconsistent sample depths, as the Niskin bottle was pulled downcurrent during the process of lowering the sampling bottle to the reef flat. Attempts to compensate, coupled with the drift of the sampling vessel resulted in the bottle "bouncing" off the bottom and likely disturbing bottom sediment. Although the bottle was left in the open position for an additional 5 seconds following any bottom contact to allow for the clearing of material, bottom contact likely led to inconsistencies in measurement.

Importantly, measurements taken using a sampling bottle are inherently discrete, sampling at a particular depth and time. Ideally, three or more samples should have been taken simultaneously to provide information on sampling variability. Given the current state of the data, it is impossible to discern sampling error from procedural error.

There are two lessons that the author took from the failure of this experiment. The first is the importance of experimental design. Even within the context of a relatively simple experiment such as this, procedural error may have been very large. Sampling should have occurred over a longer period of time in order to gather data about changes that take place over several hours (i.e. an entire tidal cycle or encompassing a solar radiance maximum and minimum. Water samples should also have been taken more frequently or in quick succession to minimize variability of the sample. The second lesson was that there are many benefits to the use of the ADCP. The instrument is not subject to the same sample variability, in terms of ocean conditions, as the water sampling procedure, assuming proper anchoring of the ADCP. In addition, and most importantly, the ADCP is able to sample over a continuous period of time and across all depth in the water column. As stated earlier, this is considerably more difficult, if not impossible to achieve using traditional water sampling techniques. The major shortcoming of ADCP data is that they provide physical parameterized data without any information regarding other characteristics in the field, such as the SPM composition or size distribution. The strengths and weaknesses can be seen in this paper: a number of physical forces were identified as influential to SPM concentrations while only hypotheses were provided about the actual characteristics of SPM.

Chapter 7: Concluding Remarks

The reef flat environment that runs the length of Kaneohe Bay is influenced by a number of different forces that can affect turbidity levels. Site location relative to the surf zone appears to be responsible for the overall level of DAEI. Currents appear to be responsible for the high-frequency variations (less than 24 hours) in DAEI. There was a strong covariant relationship at Sites 1 and 2 between vertical currents and DAEI. These vertical current appear to be a result of the incoming tide and its associated horizontal velocities. The strong relationship between vertical currents and DAEI was not present at all of the study sites. Another possible, although less likely, explanation of DAEI variations, was a diurnal migration of biological organisms.

Future work of this nature should combine chlorophyll sensors and sediment traps with ADCP measurements to determine the nature and size of the particles responsible for the EI signal. Data regarding the composition of the SPM found at Sites 1 and 2 would help to determine whether biological activity is responsible for the changes observed in the DAEI data. Attempts to calibrate echo intensity were unsuccessful due to the high temporal and spatial variability that is inherent to the reef environment. In future calibration attempts, water samples should be obtained in closer proximity to the ADCP and at a higher sampling rate.

It is this researcher's hope that this study can help others to understand the reef flat dynamics of Kaneohe Bay.

Appendix 1

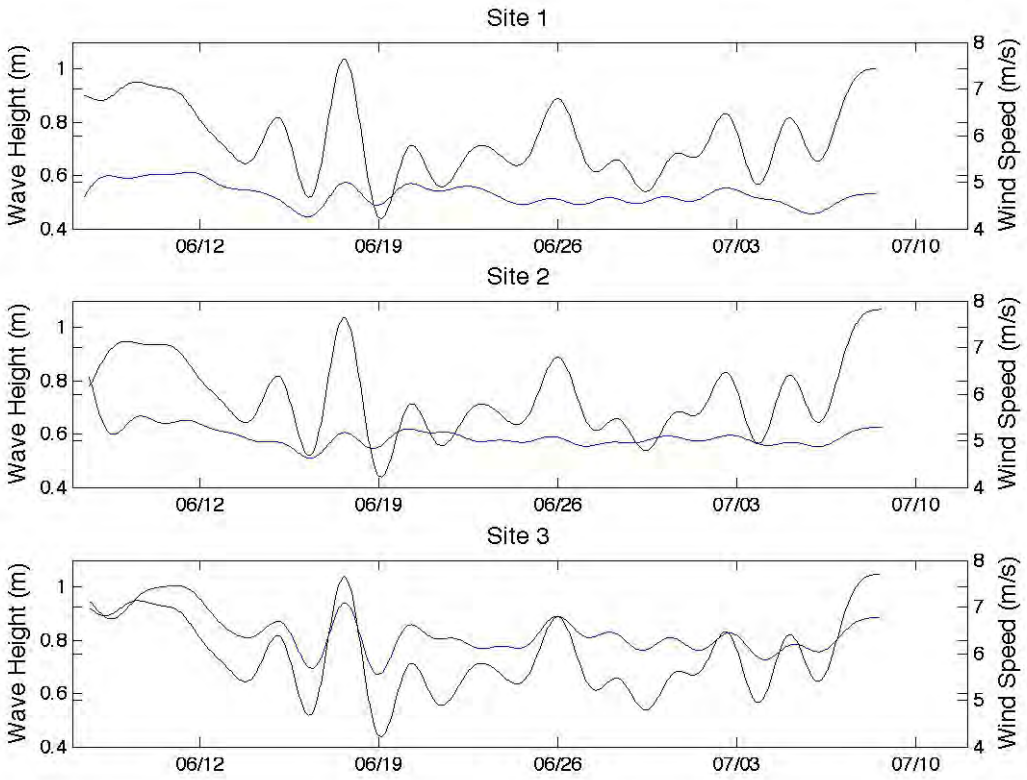

Relationship between wind speed and wave height for Deployment 2. Wave data (—) and wind data (—) have been 24-hour low-pass filtered. All sites show an expected normal relationship between wind speed and wave height. Site 3 exhibits the strongest relationship between wind and wave height, although this is partially due to the scaling of the larger wave heights at the site. Start and end points of the filter should be ignored due to errors in filter computation.

Appendix 2

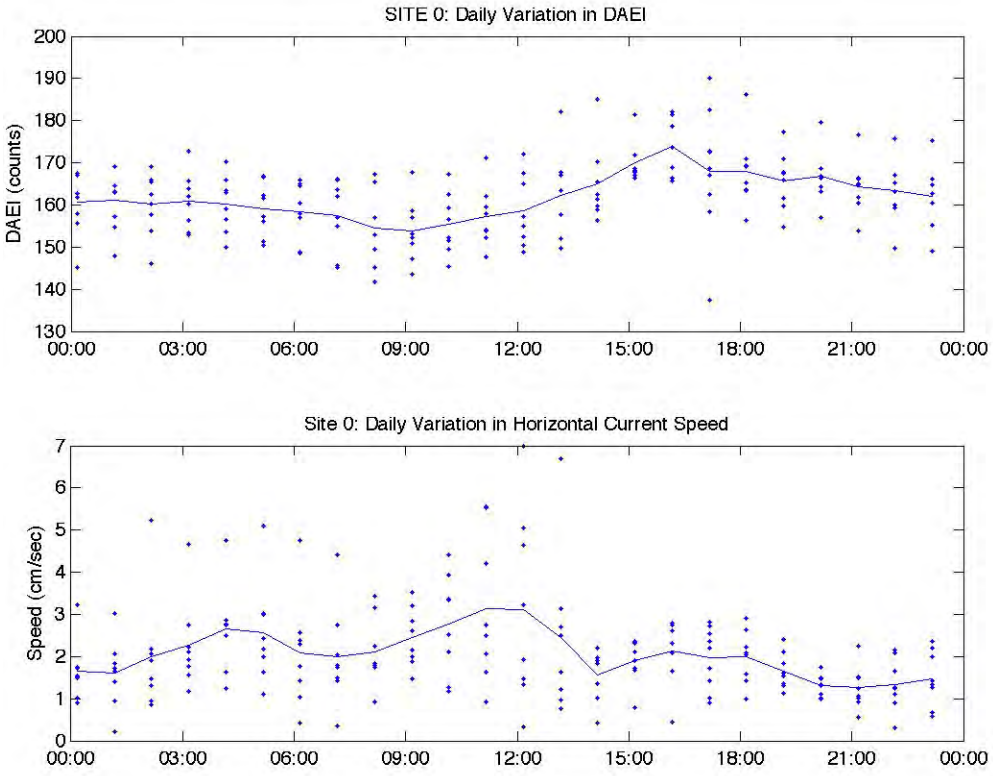

Plots of daily variations in DAEI and current speed found at Site 0 during Deployment 1. Data sampled hourly. A peak is clearly visible in the DAEI, reaching a maximum at 16:00. This maximum lags the maximum observed at Sites 1 and 2 by 2.5 hours. There appears to be no diel pattern present in horizontal current speeds.

Appendix 3

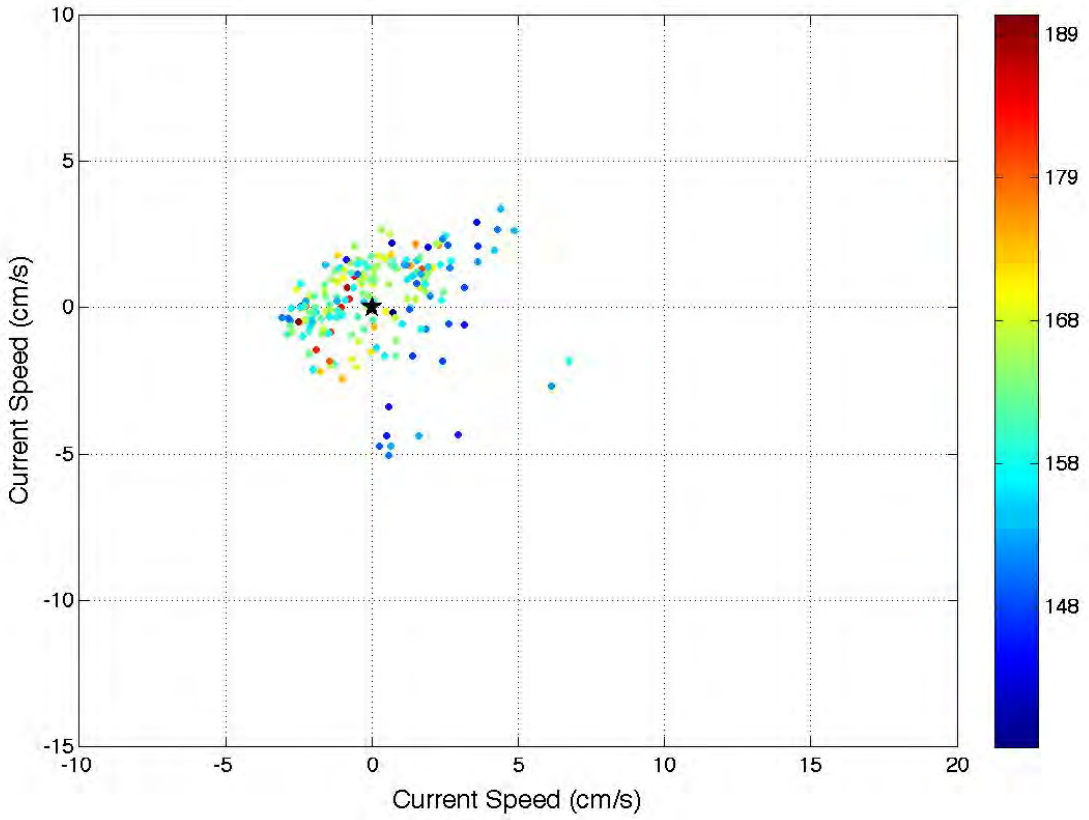

Plot of horizontal current velocities for Site 0. Each datum corresponds to the speed and direction at each sampled time, relative to the origin. Echo intensity is plotted as each point's color index, coinciding at its respective time. Site 0 exhibits horizontal currents that have a larger distribution of direction. The plot data could be interpreted to suggest a NE-SW flow direction, however, there are not enough data to establish this relationship.

Appendix 4

Site 1

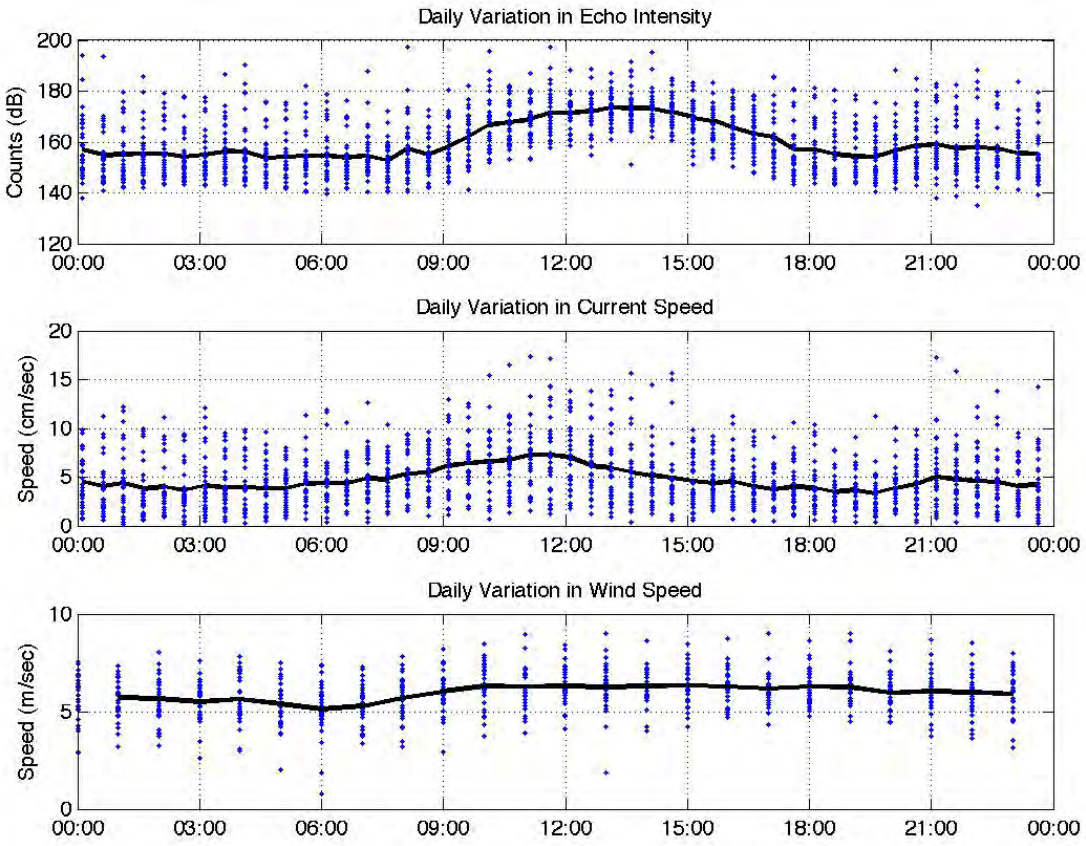

Plots of daily variations in DAEI, horizontal current speed, and wind speed observed at Site 1. Unlike DAEI, the current and wind data show little diurnal cycle. A peak in current speed at 11:30 is present, however the distribution of currents at that time follow the same range of values as those observed at other times throughout the day. There also appears to be a slight rise in daily wind speed from 7:00 to 10:00, but this was not deemed pertinent to the DAEI analysis.

Site 2

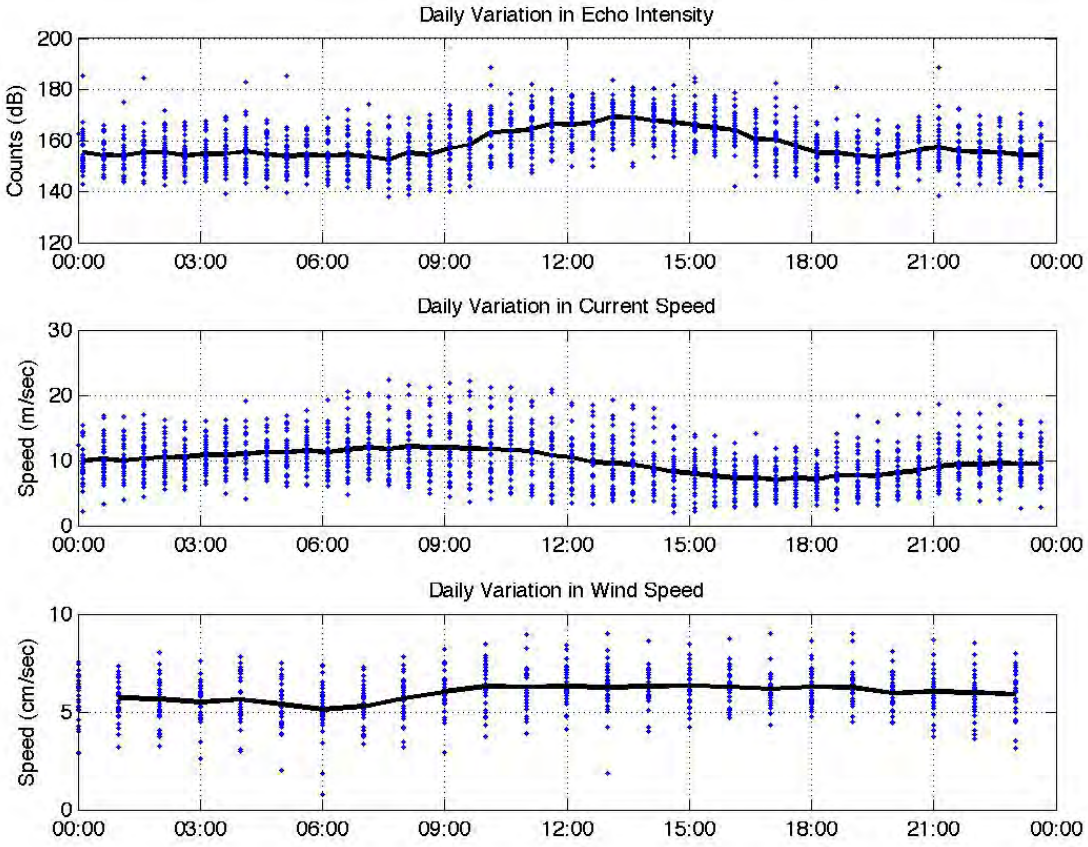

Plots of daily variations in DAEI, horizontal current speed, and wind speed observed at Site 2. Unlike DAEI, the current and wind data show little diurnal cycle. There are minimal variations in the average current speed over the course of the day.

Site 3

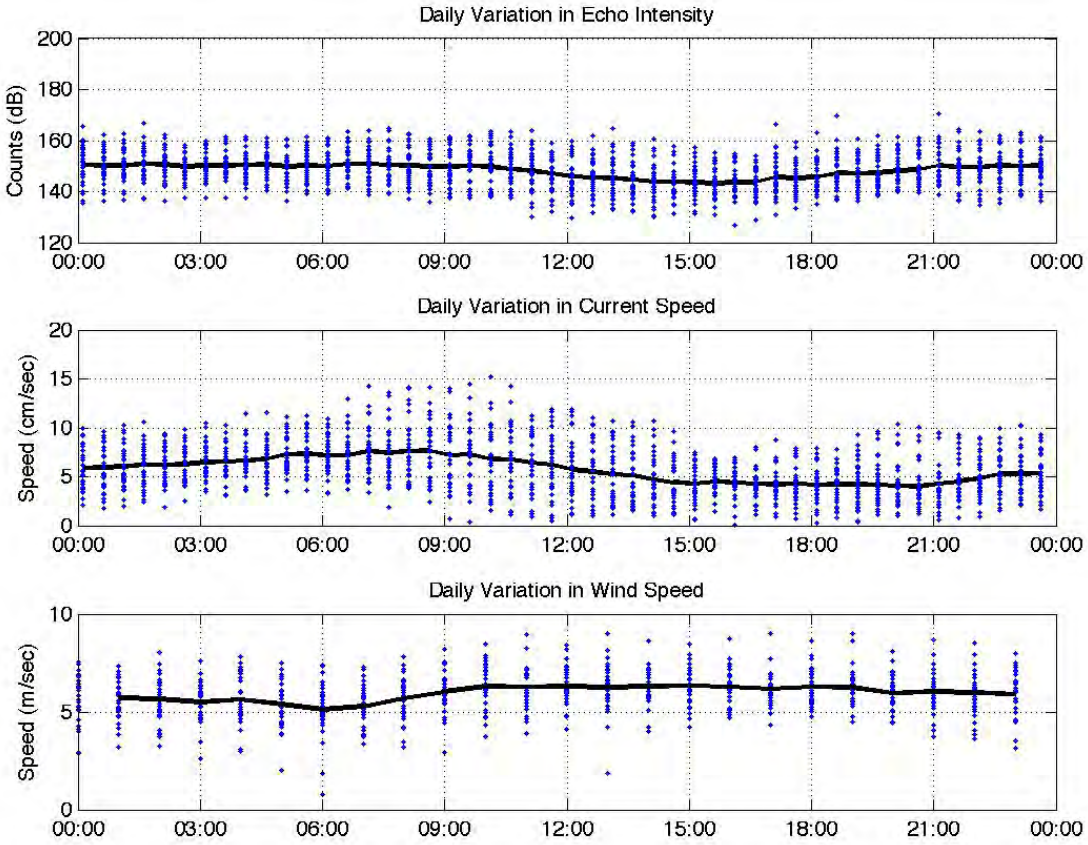

Plots of daily variations in DAEI, horizontal current speed, and wind speed observed at Site 3. Site 3 exhibits no diurnal cycle, like those seen at Sites 1 and 2. Horizontal currents vary minimally over the course of the day.

Appendix 5

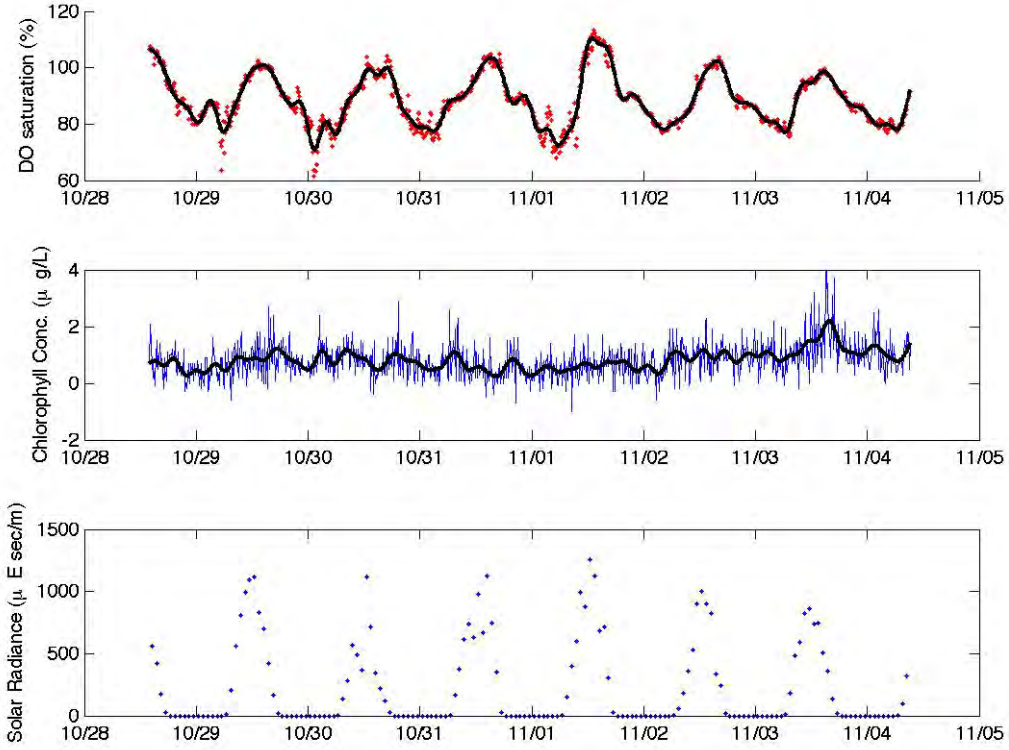

This figure shows the results from a 5-day dataset from the CRIMP buoy, positioned at the Lilipuna Channel in south Kaneohe Bay (De Carlo, unpublished). DO saturation and chlorophyll concentrations were sampled every 10 minutes and solar radiance was sampled hourly from Mokuloe Island. The (—) line represents a 6-hour low-pass filter of the data that serve to establish general low-frequency trends in the data while removing high-frequency variations. Note the synchronization between filtered DO saturation and solar radiance and the lack of this relationship in the filtered chlorophyll data. This data suggest that chlorophyll, and thus phytoplankton remains in the water column, contrary to the results of DAEI analysis.

References

Bathen, K.H. (1968). *A descriptive study of the physical oceanography of Kaneohe Bay, Oahu, Hawaii.* University of Hawaii, Hawaii Institute of Marine Biology. Tech. Report 14. 353 pp.

Deines, K.L. (1999). Backscatter estimation using broadband acoustic Doppler current profilers. *Oceans 99 IEEE Conference Proceedings, San Diego, CA*. 5 pp.

Grigg, R.W. and Dollar S.J. (1990). Natural and anthropogenic disturbances on coral reefs. In Dubinsky, Z. (Ed.) *Ecosystems of the World 25: Coral reefs*. Elsevier, Amsterdam: 439-452.

Gordon, R.L. (1996). *Acoustic Doppler Current Profiler Principles of Operation: A Practical Primer*. 2nd Edition for Broadband ADCPs. 57 pp.

Hoitink, A.J.F. (2004). Tidally-induced clouds of suspended sediment connected to shallow-water coral reefs. *Marine Geology*. 208: 13-31.

Holdaway, G.P., Thorne, P.D., Flatt, D., Jones, S.E., Prandle, D. (1999) Comparisson between ADCP and transmissometer measurements of suspended sediment concentration. *Continental Shelf Research.* 19: 421-441.

Komar, P.D. (1998). *Beach Processes and Sedimentation*. Prentice Hall, Upper Saddle River, N.J. 544 pp.

Komar, P.D. and Gaughan M.K. (1972). Airy wave theory and breaker height prediction. *Proceedings of the 13th Conference on Coastal Engineering, ASCE*: 405-418.

Moberly R, Jr. and Chamberlain T. (1964). Hawaiian beach systems. *Hawaii Institute of Geophysics Report HIG-64-2*: 15-19.

Orpin, A.R. *et al*. (2004). Natural turbidity variability and weather forecasts in risk management of anthropogenic sediment discharge near sensitive environments. *Marine Pollution Bulletin*. 49: 602-612.

Shimada, K.M. (1973). A comparison of storm-wave and tradewind-wave energies off Kaneohe Bay, Oahu, Hawaii. Department of Oceanography Masters Thesis, University of Hawaii: 115 pp.